

# A Fundamental Relation Between Supermassive Black Holes and Their Host Galaxies

Laura Ferrarese<sup>1</sup>

University of California, Los Angeles, CA, 90095, laura@astro.ucla.edu

David Merritt

Rutgers University, New Brunswick, NJ, 08854, merritt@physics.rutgers.edu

*Submitted to the Astrophysical Journal Letters*

## ABSTRACT

The masses of supermassive black holes correlate almost perfectly with the velocity dispersions of their host bulges,  $M_{BH} \propto \sigma^\alpha$ , where  $\alpha \sim 5$ . The relation is much tighter than the relation between  $M_{BH}$  and bulge luminosity, with a scatter no larger than expected on the basis of measurement errors alone.

## 1. Introduction

After decades of indirect and circumstantial evidence, the motion of gas and stars on parsec scales has provided irrefutable dynamical evidence for the presence of  $10^7 - 10^9 M_\odot$  black holes (BHs) in about a dozen elliptical and a handful of spiral galaxies (Kormendy & Richstone 1995). While efforts to build a larger, statistically significant sample continue, we have now moved from debating the existence of supermassive BHs, to asking what regulates their formation and evolution, and how their presence influences, and is influenced by, their host galaxies.

In an early review based on eight detections, Kormendy & Richstone (1995) found that the BH masses  $M_{BH}$  scale linearly with the absolute blue luminosity  $B_T^0$  of the host bulge or elliptical galaxy. This correlation was later strengthened by Magorrian et al. (1998) using a larger ( $\sim 30$ ) sample of galaxies to which simple stellar dynamical models were applied. At the same time, it has been noted (e.g. Jaffe 1999) that the  $M_{BH} - B_T^0$  relation suffers not only from severe observational biases, but also from a large scatter which is not accounted for by the uncertainties in the individual measurements. A large intrinsic scatter would hardly be surprising, given that the luminosity of the stellar component is influenced by a variety of processes that are oblivious to the events taking place in the nuclear regions, such as star formation and tidal truncation.

---

<sup>1</sup>Current Address: Department of Physics and Astronomy, Rutgers University, New Brunswick, NJ 08854

By understanding how the properties of the BHs relate to those of their host galaxies, we can hope to learn about the formation and evolution of both. In this Letter, the connection between BH masses and the stellar velocity dispersion of the host galaxy is investigated for the first time. We find a remarkably tight correlation with negligible intrinsic scatter when using galaxies with well-determined BH masses (roughly speaking, those galaxies in which the observations have resolved the sphere of gravitational influence of the BH). Our results suggest that the stellar velocity dispersion, rather than the luminosity, of a hot stellar system may be a more fundamental parameter regulating the evolution of supermassive black holes in galaxies.

## 2. Database

All BH mass estimates available to date, together with a compilation of properties of their host galaxies, are given in Table 1. Revised Hubble and T-type (from the Third Reference Catalogue, RC3, de Vaucouleurs et al. 1991) are found in columns 2 and 3, while column 4 lists distances to the host galaxy. With a few exceptions detailed in the footnotes, all distances are from surface brightness fluctuation (SBF) data (Tonry et al. 2000) calibrated as in Ferrarese et al. (2000).

Total apparent magnitudes  $m_B$ , uncorrected for Galactic absorption, are from the RC3 for all elliptical galaxies (T-type =  $-4$  or smaller), and from de Vaucouleurs & Pence (1978) for the Milky Way. For the lenticular and spiral galaxies (T-type =  $-3$  and larger),  $m_B$  for the bulge is derived by subtracting the disk contribution from the RC3 magnitude of the entire galaxy. A direct measurement of the former, derived by decomposing the galaxies’ surface brightness profile into separate bulge and disk components, is available only for NGC 224 and NGC 4594 (Simien & de Vaucouleurs 1986). The same authors define an empirical correlation between T-type and the ratio between bulge and total luminosity, which we adopt in all other cases. Because of the large intrinsic scatter ( $\sim 1$  mag) of this correlation, a 0.5 mag error has been associated with the bulge magnitudes derived in this way. Finally, all magnitudes are corrected for Galactic extinction using the DIRBE/IRAS maps of Schlegel et al. (1998) and an extinction law following Cardelli, Clayton & Mathis (1989), and converted to absolute magnitudes (column 5) given the distances in column 4.

The methods used in deriving the BH masses, and references to the original papers are listed in the last column of Table 1. Because the masses depend linearly on the assumed distance to the host galaxies, the values in column 6 have been corrected to adhere to our homogeneous set of distances. This correction is random in nature, and generally negligible, except for IC 1459, N4203, N3079 and N1068 for which our improved distances are 60% to 100% larger than quoted in the original papers. Uncertainties in the host galaxies’ distances have been incorporated in the errors in the BH masses.

The velocity dispersions  $\sigma$  given in column 7 are mostly from Davies et al. (1987), and other

papers listed in the footnotes. Different authors use apertures of different sizes for the dispersion measurements. Therefore,  $\sigma$  does not sample the same physical size in every galaxy in our sample. This introduces a potential bias, since  $\sigma$  varies with radius within the same galaxy (e.g. Tonry 1983). Quantifying this bias is complicated since the ordered rotational velocity is also folded into measurements of the central velocity dispersion; furthermore,  $\sigma$  is weighted by the galaxy’s surface brightness profile within the aperture. Jorgensen et al. (1995) used dynamical models for early type galaxies to characterize the dependence of  $\sigma$  on aperture size. We adopt Jorgensen’s prescription to correct all velocity dispersions in Table 1 to the equivalent of a  $110 \times 290 \text{ pc}^2$  aperture, corresponding to  $4'' \times 1''.5$  (the aperture used for most of the data) at a distance of 15 Mpc (representative of our sample). The correction is a few  $\text{km s}^{-1}$  for most galaxies, reaching  $\sim -30 \text{ km s}^{-1}$  (10%) only for a few distant galaxies (e.g. NGC 4889, NGC 6166, NGC 6251). The aperture-corrected  $\sigma_c$  are listed in column 8 of Table 1, and will be used in the remainder of this paper.

Finally, for the Milky Way, we use the mean velocity dispersion compiled by Kent (1992) between 0 and 90 pc, equivalent to our standard aperture.

### 3. Analysis

We did not make any attempt to homogenize the error estimates on the BH masses. Except for adding in quadrature the (small) uncertainty in the galaxies’ distances, the errors on  $M_{BH}$  listed in Table 1 are those quoted by the respective authors. However, the real uncertainties are often much larger. For instance, the Magorrian et al. (1998) mass estimates are based on fitting a simple class of dynamical models to ground-based kinematical data. In almost all of these galaxies, the data can equally well be fit by a more general class of stellar-dynamical models with no BH at all; thus the Magorrian et al. mass estimates might conservatively be interpreted as upper limits (e.g. van der Marel 1997). The same is true for the majority of ground-based, stellar-kinematical BH detections.

In view of this fact, we divide the galaxies in Table 1 into three subsamples based purely on the reliability of their BH mass estimates. The proper motion studies of the Sagittarius A star cluster and the dynamics of the water maser disk in NGC 4258 lead to the most robust determinations of  $M_{BH}$ . Close seconds are estimates in 10 additional galaxies, based on data from high-resolution HST observations, either absorption-line stellar spectra or observations of the motion of nuclear dust/gas disks. These 12 galaxies comprise our “Sample A.” The BH mass in Arp 102B, obtained from fitting accretion disk models to variable optical emission lines, and BH mass estimates based on stellar kinematics obtained from the ground (i.e. the Magorrian et al. 1998 sample) define our “Sample B.” BH masses published as upper limits are listed separately in Table 1 and are not considered further.

We then searched for linear correlations between  $\log M_{BH}$  and both  $B_T^0$  and  $\log \sigma_c$ . Since both

the dependent and independent variables suffer from non-negligible measurement uncertainties, we used the bivariate linear regression routine of Akritas & Bershadsky (1996), which accommodates intrinsic scatter as well as measurement errors in both variables.  $M_{BH}$  was taken as the dependent variable. The results of the regression fits are summarized in Table 2 and Figure 1.

The correlation between  $M_{BH}$  and bulge magnitude  $B_T^0$  (Fig. 1a,c) is poor, both for Sample A and Sample B. Although the best linear fit to the data has a slope close to the value of  $-0.4$  expected if  $M_{BH}$  is simply proportional to  $M_{bulge}$ , it is apparent from the figure, and from the reduced  $\chi_r^2$  of the fit (Table 2), that even by restricting the sample to the galaxies with the most accurately determined BH masses, the intrinsic scatter in the  $M_{BH} - B_T^0$  relation remains significantly larger than the reported errors. No sub-sample of galaxies, selected either by Hubble Type or method used in deriving  $M_{BH}$ , defines a tight linear relation between  $M_{BH}$  and  $B_T^0$ . This implies that differences in the mass-to-light ratio between Hubble types, or systematic biases affecting any particular method, are unlikely to account for the large scatter.

Figures 1b and 1d show the dependence of  $M_{BH}$  on the central stellar velocity dispersion  $\sigma_c$  of the host bulge or elliptical galaxy. The correlation is remarkable: Sample A, which shows a large scatter in the  $M_{BH} - B_T^0$  plots, now defines a linear relation with negligible intrinsic scatter. The best-fit linear relation is

$$\log M_{BH} = 5.27(\pm 0.40) \log \sigma_c - 4.04(\pm 0.95) \quad (1)$$

with  $M_{BH}$  in units of  $M_\odot$  and  $\sigma_c$  in  $\text{km s}^{-1}$ . There is no evidence for the existence of a second parameter: the reduced  $\chi^2$  of the fit (Table 2) is only 0.43, consistent with a scatter that derives entirely from measurement errors; in fact such a low value may indicate that the errors in  $M_{BH}$  have been slightly overestimated. The first incarnation of Equation (1) was suggested by Merritt (2000) based on the values of  $M_{BH}$  and  $\sigma$  for M84, M87 and NGC 4258.

By contrast, the galaxies in Sample B define a much weaker correlation between  $M_{BH}$  and  $\sigma_c$  (Fig. 1d). Furthermore, the BH masses in this sample lie systematically above the mean line defined by Sample A, with a mean offset of a factor  $\sim 3$ . Since the two samples were chosen purely on the basis of the reliability of the  $M_{BH}$  estimates, it seems likely that the poorer correlation in Sample B results mostly from errors in the determination of  $M_{BH}$  for these galaxies.

Before proceeding any further we comment on the possibility that the slope of the  $M_{BH} - \sigma$  relation might suffer from observational biases. Many authors (e.g. Jaffe et al. 1999) have remarked that the  $M_{BH} - B_T^0$  relation might represent the upper envelope of a wedge shaped distribution, since BHs with small masses would escape detection in very luminous galaxies. The same bias affects the  $M_{BH} - \sigma$  relation, since the radius of influence of the BH decreases as the inverse square of the stellar velocity dispersion. On the other hand, to our knowledge, there are no giant ellipticals which have been searched for a BH and for which a detection, or upper limit, inconsistently smaller than predicted by our  $M_{BH} - \sigma$  relation has been found. Furthermore, the small scatter of the  $M_{BH} - \sigma$  relation suggests that any such observational bias is likely to be slight.

A linear fit to Sample A using velocity dispersions uncorrected for the effect of aperture size instead of  $\sigma_c$  (column 7 of Table 1) produces an equally tight relation, but with a slightly shallower slope:  $4.80 \pm 0.50$ . Corrections for aperture size are negative for galaxies at large distances, and positive for nearby galaxies (e.g. N221 and NGC 4258). Because of selection effects, distant galaxies tend to be the most luminous and have the largest velocity dispersions, while NGC 4258 and M32 are at the opposite end of the distribution. Correcting for aperture size will therefore steepen the  $M_{BH} - \sigma$  relation, as observed. A larger, volume-limited sample of galaxies is needed to assess the exact magnitude of this (small) bias.

A more serious concern is whether the tight correlation between  $M_{BH}$  and  $\sigma$  might simply reflect the influence of the BH on the stellar kinematics of the nucleus, i.e. perhaps  $M_{BH}$  and  $\sigma$  are simply different measures of the BH mass. However, the influence of the BH on  $\sigma$  must generally be small, for several reasons. First, if the gravitational force of the BH were dominating the observed kinematics, one would expect a relation  $M_{BH} \sim \sigma^2$ , much flatter than observed. Second, most of the observations of  $\sigma$  listed in Table 1 were carried out using apertures much larger than the expected radius of gravitational influence of the BH; the latter is typically much less than  $1''$ . While the BH would certainly be expected to increase the luminosity-weighted value of  $\sigma$  measured within a centered aperture, the effect is likely to be slight. We may verify this in the case of M32, for which Table 1 gives  $\sigma = 80 \text{ km s}^{-1}$  and  $\sigma_c = 90 \text{ km s}^{-1}$ . The velocity dispersion profile and rotation curve of M32 are now available via HST at a resolution of  $\sim 0''.1$ , and the BH is observed to influence the stellar kinematics only within  $\sim 0''.3$  (Joseph et al. 2000). Based on the data in that paper, we find that an aperture centered on the BH but excluding this inner region would yield an rms velocity that lies between  $\sim 80$  and  $\sim 90 \text{ km s}^{-1}$  for any outer aperture radius smaller than  $\sim 5''$ . Thus, the tabulated  $\sigma$  for M32 is essentially unaffected by the presence of the BH. Most of the galaxies in our sample have shallower brightness profiles than M32 and were observed with lower effective resolution; hence we expect their  $\sigma$  values to be even less influenced by their BHs.

But the most convincing evidence that we are seeing a true correlation between BH mass and the properties of the stellar bulge is presented in Figure 2. Here we have plotted  $M_{BH}$  vs. a measure of the rms stellar velocity at a radius of  $r_e/4$ , with  $r_e$  the effective radius. This is much greater than the radius at which the BH could have a measurable effect on the stellar velocities. As a measure of the rms velocity we took  $v_{rms} = \sqrt{(\sigma^2 + v_r^2 / \sin^2 \theta)_{r_e/4}}$ , with  $\sigma$  and  $v_r$  the measured stellar velocity dispersion and mean line-of-sight velocity. Values of  $\sigma$  and  $v_r$  are readily available in the literature (e.g. Prugniel et al. 1998; McElroy 1995). The inclination angle  $\theta$  between the rotation axis and the line of sight, however, is seldom well determined; in fact, estimates are available only for NGC 3115 (Emsellem et al. 1999) and NGC 4342 (Scorza & van den Bosch 1998). Neglecting the  $\sin \theta$  term is inconsequential for the slowly rotating giant ellipticals (assuming the slow rotation is not a consequence of the galaxy being viewed face-on), but  $v_{rms}$  for the rapidly rotating NGC 221 and NGC 3379, plotted as crosses in Figure 2, should be taken as lower limits. Linear regression fits (Table 2) show that the slopes of  $M_{BH}$  vs bulge

velocity are coincident, within their respective errors, whether  $\sigma_c$  or  $v_{rms}$  is used. Besides the Milky Way, for which  $r_e$ ,  $\sigma$  and  $v_r$  are rather uncertain (Heraudeau & Simien 1998), the only galaxy that deviates significantly from the relation is NGC 4486 (M87). The discrepancy is in the sense expected if the galaxy is rotating with  $v_r \sim 270 \text{ km s}^{-1}$  around a rotation axis aligned with the line of sight.

We stress that – even if the correlation between  $M_{BH}$  and  $\sigma_c$  is due in part to the gravitational influence of the BH on the motion of stars in the nucleus – this would not vitiate the usefulness of the relation as a predictor of  $M_{BH}$ . *Figure 1b suggests that  $M_{BH}$  can be predicted with an accuracy of  $\sim 50\%$  or better from a single, low-resolution observation of a galaxy’s velocity dispersion.* This is a remarkable result.

#### 4. Discussion

We have found a nearly perfect correlation between the masses of nuclear BHs and the velocity dispersions of their host bulges,  $M_{BH} \propto \sigma^\alpha$ , where  $\alpha \approx 5$ . Here we examine some of the implications of this correlation.

Almost all of the BH mass estimates in Table 1 that were derived from ground-based, stellar kinematical data fall above the tight correlation defined by our Sample A (Fig. 1d), some by as much as two orders of magnitude. Why should this be? We propose the following explanation. The fit of a stellar dynamical model to a set of data can almost always be improved by adding a free parameter to the potential in the form of a central point mass. However if the data are too poor to resolve the BH’s sphere of influence, only values of  $M_{BH}$  that are larger than the true BH mass will significantly affect the  $\chi^2$  of the model fit. Hence one expects to see a bias toward overly-large values of  $M_{BH}$  when modeling low-resolution data. We believe that this is the case with the majority of the Magorrian et al. (1998) mass estimates; as supporting evidence, we note that the most distant galaxies in their sample (NGC 1600, 2832, 4874, 4889, 6166, 7768) are among those with the most discrepant masses in Figure 1d. We predict that these galaxies will turn out to have BH masses that are too small to be usefully constrained by currently existing data. We also suggest that correlation studies based on the Magorrian et al. mass estimates (e.g. Merrifield, Forbes & Terlevich 2000) should be interpreted with caution.

The  $M_{BH} - \sigma$  relation may be used to predict the masses of BHs in galaxies where the data currently provide only weak constraints or upper limits. We list some predictions below, based on the velocity dispersions in Table 1 (in the case of M33 we used the Kormendy & McClure 1993 measurement,  $\sigma = 21 \text{ km s}^{-1}$ ).

$$\text{M31: } 3.4 \times 10^7 M_\odot$$

$$\text{M33: } 8.5 \times 10^2 M_\odot$$

$$\text{NGC 4486B: } 4.9 \times 10^7 M_\odot$$

NGC 4874:  $2.0 \times 10^8 M_\odot$

Our prediction for  $M_{BH}$  in M31 is somewhat lower than the most recent determination by Bacon et al. (1994) ( $\sim 6 \times 10^7 M_\odot$ ) but consistent with the earlier estimate of Dressler & Richstone (1988). For M33, Kormendy & McClure (1993) found  $M_{BH} < 5 \times 10^4 M_\odot$ . If our estimate of  $M_{BH}$  is correct, the radius of influence of this BH is only  $\sim 0.01\text{pc} \sim 0''.003$ , which is below the resolution limit of even the Space Telescope Imaging Spectrograph. In the case of NGC 4486B, our predicted mass is an order of magnitude smaller than the Kormendy et al. (1997) estimate. Finally, our prediction for  $M_{BH}$  in NGC 4874 is a full two orders of magnitude smaller than the Magorrian et al. (1998) determination; if our value is correct, the radius of gravitational influence of this BH is only  $\sim 15\text{pc} \sim 0''.03$ , far too small to have been resolved from the ground. We note in passing that significant efforts have been made to constrain the mass of a (putative) BH in the core-collapsed globular cluster M15 (van der Marel 2000; Gebhardt et al. 2000), giving an upper limit of  $\sim 2000 M_\odot$ . Equation 1 predicts  $M_{BH} < 150 M_\odot$ , by conservatively assuming  $\sigma_c < 14 \text{ km s}^{-1}$  (van den Marel 2000). However, we caution against the indiscriminate extrapolation of Equation 1 much below the range plotted in Figure 1, as the formation mechanism of BHs with masses smaller than  $\sim 10^5 M_\odot$  might differ from that of more massive systems (Haehnelt, Natarajan & Rees 1999).

Why should BH masses be so tightly correlated with bulge velocity dispersions? One possibility is a fundamental connection between  $M_{BH}$  and the stellar mass of the bulge, with  $\sigma$  a good predictor of bulge mass – a better predictor, for instance, than  $B_T^0$ . This explanation is superficially plausible, since the masses of early-type galaxies scale with their luminosities as  $M \sim L^{5/4}$  (Faber et al. 1987) and  $L \sim \sigma^4$ , hence  $M \sim \sigma^5$ . The  $M_{BH} - \sigma$  relation of Figure 1b would therefore imply a rough proportionality between BH mass and bulge mass, i.e. that a universal fraction of the baryonic mass was converted into BHs (Haiman & Loeb 1998). Such a relation could be maintained in spite of mergers if the gas mass accreted by the BHs during the merger were a fixed fraction of the gas mass converted into stars (Cattaneo, Haehnelt & Rees 1999).

Another possibility is that  $\sigma$  measures the depth of the potential well in which the BH formed. A number of authors (Wang & Biermann 1998; Silk & Rees 1998; Haehnelt, Natarajan & Rees 1999) have suggested that quasar outflows might limit BH masses by inhibiting accretion of gas. Equating the energy liberated in one dynamical time of the bulge to the gravitational binding energy, and assuming accretion at the Eddington rate, gives a maximum BH mass that scales as  $\sigma^5$  (Silk & Rees 1998), again consistent with the observed relation. This dependence could be maintained in the face of mergers only if BHs continued to grow by gas accretion during all stages of the merger hierarchy (Kauffmann & Haehnelt 2000).

We thank Avi Loeb for an illuminating discussion which served as a key motivation for this paper. LF acknowledges support from NASA through grant number NRA-98-03-LTSA-03, and DM acknowledges grants NSF AST 96-17088 and NASA NAG5-6037. This research has made

use of the NASA/IPAC Extragalactic Database (NED) which is operated by the Jet Propulsion Laboratory, California Institute of Technology, under contract with the National Aeronautics and Space Administration.

## REFERENCES

- Akritas, M. G. & Bershad, M. A. 1996, *ApJ*, 470, 706
- Bower, G.A., et al. 1998, *ApJL*, 492, L111 (B98)
- Cardelli, J. A., Clayton, G. C. & Mathis, J. S. 1989, *ApJ*, 345, 245
- Cattaneo, A., Haehnelt, M. G. & Rees, M. J. 1999, *MNRAS*, 308, 77
- Cretton, N., & van den Bosch, F.C. 1999, *ApJ*, 514, 704 (CB99)
- Davies, M. et al. 1987, *ApJ*, 64, 581
- de Vaucouleurs, G. & Pence, W. D. 1978, *AJ*, 83, 1163
- de Vaucouleurs, G., de Vaucouleurs, A., Corwin, H. G., Buta, R. J., Paturel, G. & Fouque, P. 1991, *Third Reference Catalog of Bright Galaxies* (New York: Springer) (RC3)
- Emsellem, E., Dejonghe, H., & Bacon, R. 1999, *MNRAS*, 303, 495 (EDB99)
- Faber, S. et al. 1987, in *Nearly Normal Galaxies*, ed. S. Faber (Springer: New York), 175
- Ferrarese, L., & Ford, H.C. 1999 *ApJ* 515, 583 (F99)
- Ferrarese, L., Ford, H.C., & Jaffe, W. 1996, *ApJ*, 470, 444 (FFJ96)
- Ferrarese, L. et al. 2000, *ApJ*, 529, 745
- Gebhardt, K., et al. 2000, *AJ*, 119, 1157 (G00)
- Gebhardt, K., et al. 2000, *AJ*, 119, 1268
- Genzel, R., et al. 2000, *astro-ph/0001428* (Ge00)
- Greenhill, L.J., Moran, J.M., & Herrnstein, J.R. 1997, *ApJL*, 481, L23 (GMH97)
- Greenhill, L.J., et al. 1996, *ApJL*, 472, L21 (G96)
- Haehnelt, M. G., Natarajan, P. & Rees, M. J. 1998, *MNRAS*, 300, 817
- Haiman, Z., & Loeb, A. 1998, *ApJ*, 505, 517
- Heraudeau, Ph. & Simien, F. 1998, *A&AS*, 136, 509
- Herrnstein, J.R., et al. 1999, *Nature*, 400, 539
- Huchra, J., & Mader, J. 1998, <http://cfa-www.harvard.edu/~huchra>, ZCAT Version July 15, 1998
- Jaffe, W. 1999, in *Galaxy Dynamics*, *Astron. Soc. Pac. Conf. Ser. Vol 182* (ed. D. Merritt, J. A. Sellwood & M. Valluri), p. 13
- Joseph, C., et al. 2000, *ApJ*, in press (*astro-ph/0005530*)



- Jorgensen, I., Franx, M. & Kjaergaard, P. 1995, MNRAS, 276, 1341
- Kauffmann, G. & Haehnelt, M. 2000, MNRAS, 311, 576
- Kent, S. 1992, ApJ, 387, 181
- Kormendy, J., et al. 1997, ApJL, 482, L139
- Kormendy, J. & McClure, R. D. 1993, AJ, 105, 1793
- Kormendy, J. & Richstone, D. O. 1995, ARAA, 33, 581
- Macchetto, F., et al. 1997, ApJ, 489, 579 (M97)
- Madore, B. F., & Freedman, W. L. 1991, PASP, 103, 933
- Magorrian, J. et al. 1998, AJ, 115, 2285
- McElroy, D.B. 1995, ApJS, 100, 105
- Merrifield, M. R., Forbes, D. A. & Terlevich, A. I. 2000, astro-ph/0002350
- Merritt, D. 2000, in Dynamics of Galaxies: from the Early Universe to the Present, Eds.: F. Combes, G. A. Mamon, and V. Charmandaris, ASP Conference Series, Vol. 197, p. 221.
- Miyoshi, M. et al. 1995, Nature, 373, 127 (M95)
- Newman, J.A., et al. 1997, ApJ, 485, 570 (N97)
- Prugniel, Ph., Zasov, A., Busarello, G. & Simien, F. 1998, A& A, 127, 117 (P98)
- Schinnerer, E., et al. 2000, ApJ, 533, 850 (Sc00)
- Schlegel, D. J., Finkbeiner, D. P. & Davis, M. 1998, ApJ, 500, 525
- Scorza, C. & van den Bosch, F. C. 1998, MNRAS, 300, 469
- Shields, J.C., et al. 2000, astro-ph/0004047 (S00)
- Silk, J. & Rees, M. J. 1998, A& A, 331, L4
- Simien, F. & de Vaucouleurs, G. 1986, ApJ, 302, 564
- Tonry, J. L. 1983, ApJ, 266, 58
- Tonry, J. L., et al. 2000, ApJS, submitted
- Trotter, A.S., et al. 1998, ApJ, 495, 740 (T98)
- van der Marel, R. P. 1997, in Galaxy Interactions at Low and High Redshift, Proc. IAU Symposium 186 (Kluwer: Dordrecht)
- van der Marel, R. P. 2000, in Black Holes in Binaries and Galactic Nuclei, eds. Kaper L., van den Heuvel E. P. J., Woudt P. A., Springer-Verlag, 2000 (astro-ph/0001342)
- van der Marel, R.P., & van den Bosch, F.C. 1998, AJ, 116, 2220 (MB98)
- Versoes Kleijn, G.A., et al. 2000, astro-ph/0003433 (VK00)
- Wang, Y. & Biermann, P. L. 1998, A& A, 334, 87

Winge, C. et al. 1999, ApJ, 519, 134 (W99)

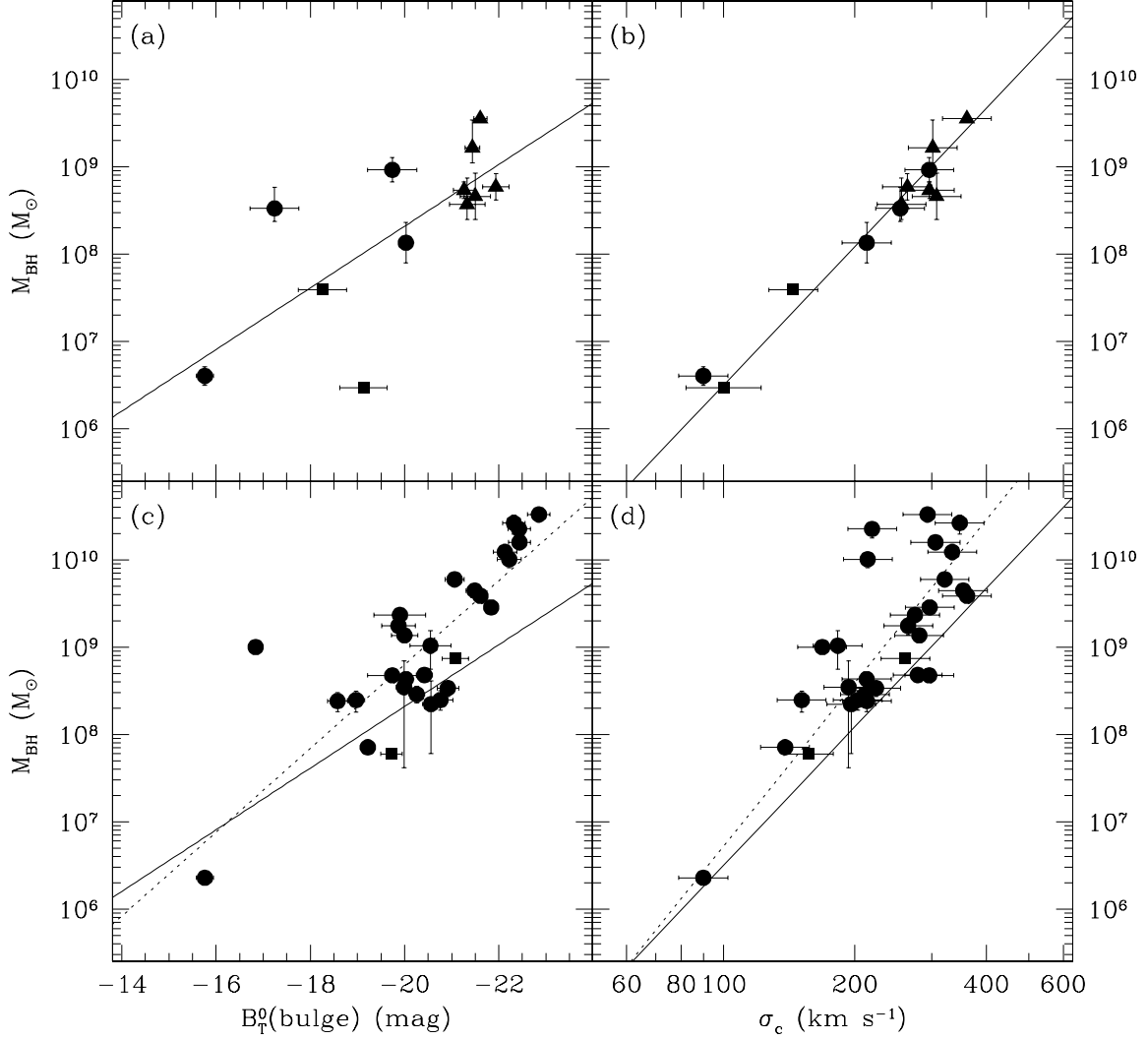


Fig. 1.— (a): BH mass versus absolute blue luminosity of the host elliptical galaxy or bulge for our most reliable Sample A. The solid line is the best linear fit (Table 2). Circles and triangles represent mass measurements from stellar and dust/gas disk kinematics respectively. The square at  $M_{BH} \sim 3 \times 10^6 M_{\odot}$  is the Milky Way (BH mass determined from stellar proper motions); the other square is NGC 4258 ( $M_{BH}$  based on water maser kinematics). The MW and NGC 4258 are the only two spiral galaxies in the sample. (b) Again for Sample A, BH mass versus the central velocity dispersion of the host elliptical galaxy or bulge, corrected for the effect of varying aperture size as described in §2. Symbols are as in panel (a). (c): Same as panel (a) but for Sample B. Circles are elliptical galaxies, squares are spiral galaxies. The solid line is the same least-squares fit shown in panel (a); dashed line is the fit to Sample B. All BH mass estimates in this sample are based on stellar kinematics. (d): Same as panel (b) but for Sample B. Symbols are as in panel (c).

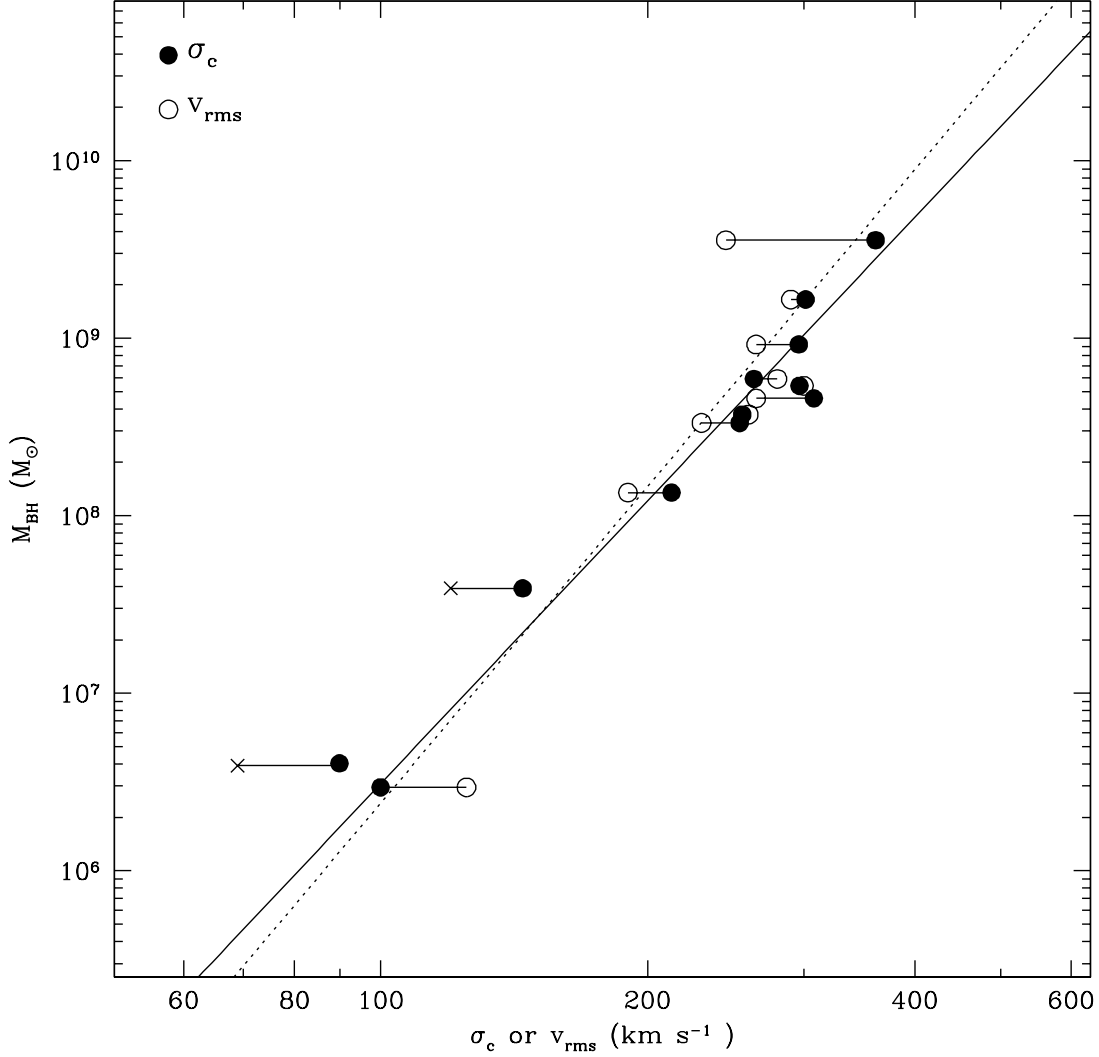


Fig. 2.— BH mass versus the central velocity dispersion  $\sigma_c$  of the host elliptical galaxy or bulge (solid circles) or the rms velocity  $v_{\text{rms}}$  measured at 1/4 of the effective radius (open circles). Crosses represent lower limits in  $v_{\text{rms}}$ . The solid and dashed lines are the best linear fits using  $\sigma_c$  (as in Figure 1b) and  $v_{\text{rms}}$  respectively.

Table 1. Database of black hole mass estimates and properties of the host galaxies

| Galaxy Name    | Rev. Hubble Type | T-type   | Distance <sup>(1)</sup> (Mpc) | $B_T^0$ (mag) | BH Mass ( $10^8 M_\odot$ )                | $\sigma^{(2)}$ (km s <sup>-1</sup> ) | $\sigma_c$ (km s <sup>-1</sup> ) | Method and References <sup>(3)</sup> |
|----------------|------------------|----------|-------------------------------|---------------|---|--------------------------------------|----------------------------------|--------------------------------------|
| • Sample A     |                  |          |                               |               |   |                                      |                                  |                                      |
| MW             | SbI-II           | ...      | 8.0±0.9 <sup>(1)</sup>        | -19.13±0.50   | 0.0295±0.0035                             | 100±20                               | 100±20                           | PM; Ge00                             |
| I1459          | E3               | -5.0±0.3 | 30.3±4.0                      | -21.50±0.32   | 4.6±2.8                                   | 322±41                               | 308±40                           | G; VK00                              |
| N221           | cE2              | -6.0±0.3 | 0.8±0.1                       | -15.76±0.18   | 0.040±0.010                               | 80±10                                | 90±12                            | G; J00                               |
| N3115          | S0 <sup>-</sup>  | -3.0±0.3 | 9.8±0.6                       | -19.74±0.52   | 9.2±3.0                                   | 291±38                               | 296±38                           | S; EDB99                             |
| N3379          | E1               | -5.0±0.3 | 10.8±0.7                      | -20.03±0.14   | 1.35±0.73                                 | 210±27                               | 213±28                           | S; G00                               |
| N4258          | SAB(s)bc         | 4.0±0.3  | 7.2±0.3                       | -18.26±0.51   | 0.3901±0.034                              | 146±19                               | 145±19                           | M; M95                               |
| N4261          | E2               | -5.0±0.3 | 33.0±3.2                      | -21.26±0.22   | 5.4 <sup>+1.2</sup> <sub>-1.2</sub>       | 306±40                               | 296±38                           | G; FFJ96                             |
| N4342          | S0 <sup>-</sup>  | -3.0±0.5 | 16.7±1.0                      | -17.24±0.52   | 3.3 <sup>+1.9</sup> <sub>-1.1</sub>       | 255±33                               | 254±33                           | S; CB99                              |
| N4374          | E1               | -5.0±0.3 | 18.7±1.2                      | -21.44±0.15   | 17 <sup>+12</sup> <sub>-6.7</sub>         | 304±39                               | 301±39                           | G; B98                               |
| N4486          | E0pec            | -4.0±0.3 | 16.7±1.0                      | -21.61±0.14   | 35.7 <sup>+2.4</sup> <sub>-2.4</sub>      | 370±48                               | 361±47                           | G; M97                               |
| N6251          | E                | -5.0±0.8 | 104±10                        | -21.94±0.28   | 5.9±2.0                                   | 293±38                               | 263±34                           | G; FF99                              |
| N7052          | E                | -5.0±0.7 | 66.1±6.4                      | -21.33±0.38   | 3.7 <sup>+2.6</sup> <sub>-1.5</sub>       | 270±35                               | 256±33                           | G; MB98                              |
| • Sample B     |                  |          |                               |               |   |                                      |                                  |                                      |
| Arp102B        | E0               | -5.0±0.5 | 101.9±9.9                     | -20.02±0.26   | 2.20 <sup>+0.29</sup> <sub>-0.73</sub>    | ...                                  | ...                              | AD; N97                              |
| N221           | cE2              | -6.0±0.3 | 0.8±0.1                       | -15.76±0.18   | 0.0228±0.0026                             | 80±10                                | 90±12                            | Sg; Mag99                            |
| N224           | SA(s)b           | 3.0±0.3  | 0.8±0.0                       | -19.72±0.23   | 0.598 <sup>+0.035</sup> <sub>-0.032</sub> | 137±18                               | 157±20                           | Sg; Mag99                            |
| N821           | E6               | -5.0±0.6 | 24.7±2.5                      | -20.76±0.27   | 2.48 <sup>+0.61</sup> <sub>-0.67</sub>    | 207±27                               | 203±26                           | Sg; Mag99                            |
| N1399          | E1pec            | -5.0±0.3 | 20.5±1.6                      | -21.06±0.20   | 60 <sup>+10</sup> <sub>-11</sub>          | 327±42                               | 321±42                           | Sg; Mag99                            |
| N1600          | E3               | -5.0±0.3 | 68.5±6.6                      | -22.44±0.23   | 159 <sup>+20</sup> <sub>-28</sub>         | 325±42                               | 306±40                           | Sg; Mag99                            |
| N2300          | S0 <sup>0</sup>  | -2.0±0.3 | 27.0±2.6                      | -19.90±0.55   | 23.3 <sup>+3.6</sup> <sub>-3.2</sub>      | 281±36                               | 274±36                           | Sg; Mag99                            |
| N2832          | E2               | -4.0±0.3 | 96.8±9.4                      | -22.13±0.25   | 123±25                                    | 360±47                               | 334±43                           | Sg; Mag99                            |
| N3115          | S0 <sup>-</sup>  | -3.0±0.3 | 9.8±0.6                       | -19.74±0.52   | 4.74 <sup>+0.35</sup> <sub>-0.38</sub>    | 291±38                               | 296±38                           | Sg; Mag99                            |
| N3377          | E5               | -5.0±0.3 | 11.6±0.6                      | -19.22±0.16   | 0.71 <sup>+0.09</sup> <sub>-0.078</sub>   | 137±18                               | 138±18                           | Sg; Mag99                            |
| N3379          | E1               | -5.0±0.3 | 10.8±0.7                      | -20.03±0.14   | 4.29 <sup>+0.41</sup> <sub>-0.59</sub>    | 210±27                               | 213±28                           | Sg; Mag99                            |
| N3608          | E2               | -5.0±0.3 | 23.6±1.5                      | -20.26±0.17   | 2.87±0.63                                 | 215±28                               | 211±27                           | Sg; Mag99                            |
| N4168          | E2               | -5.0±0.3 | 31.7±6.2                      | -20.55±0.43   | 10.4 <sup>+4.1</sup> <sub>-6.4</sub>      | 192±25                               | 183±24                           | Sg; Mag99                            |
| N4278          | E1               | -5.0±0.3 | 15.3±1.7                      | -20.00±0.28   | 13.6 <sup>+1.7</sup> <sub>-1.8</sub>      | 281±36                               | 281±36                           | Sg; Mag99                            |
| N4291          | E                | -5.0±0.5 | 26.9±4.1                      | -19.87±0.36   | 17.5 <sup>+3.6</sup> <sub>-4.2</sub>      | 271±35                               | 265±34                           | Sg; Mag99                            |
| N4472          | E2               | -5.0±0.3 | 16.7±1.0                      | -21.84±0.14   | 28.5 <sup>+4.0</sup> <sub>-5.2</sub>      | 298±39                               | 297±39                           | Sg; Mag99                            |
| N4473          | E5               | -5.0±0.3 | 16.1±1.1                      | -19.99±0.16   | 3.5 <sup>+2.4</sup> <sub>-7.5</sub>       | 194±25                               | 193±25                           | Sg; Mag99                            |
| N4486          | E0pec            | -4.0±0.3 | 16.7±1.0                      | -21.61±0.14   | 38.6 <sup>+3.4</sup> <sub>-3.5</sub>      | 370±48                               | 361±47                           | Sg; Mag99                            |
| N4486B         | cE0              | -6.0±0.6 | 16.7±1.0                      | -16.84±0.14   | 10.0 <sup>+1.4</sup> <sub>-0.98</sub>     | 169±22                               | 168±21                           | Sg; Mag99                            |
| N4552          | E0               | -5.0±0.4 | 15.7±1.2                      | -20.42±0.17   | 4.79 <sup>+0.88</sup> <sub>-0.62</sub>    | 279±36                               | 278±36                           | Sg; Mag99                            |
| N4564          | E                | -5.0±0.5 | 14.9±1.2                      | -18.97±0.18   | 2.48 <sup>+0.59</sup> <sub>-0.78</sub>    | 154±20                               | 151±10                           | Sg; Mag99                            |
| N4594          | SA(s)a           | 1.0±0.3  | 9.9±0.9                       | -21.08±0.28   | 7.39 <sup>+0.67</sup> <sub>-0.72</sub>    | 262±34                               | 261±34                           | Sg; Mag99                            |
| N4621          | E5               | -5.0±0.3 | 18.6±1.9                      | -20.92±0.23   | 3.39 <sup>+0.59</sup> <sub>-0.74</sub>    | 230±30                               | 227±29                           | Sg; Mag99                            |
| N4636          | E0               | -5.0±0.3 | 15.0±1.1                      | -20.56±0.18   | 2.2 <sup>+1.4</sup> <sub>-2.9</sub>       | 196±25                               | 196±25                           | Sg; Mag99                            |
| N4649          | E2               | -5.0±0.3 | 17.3±1.3                      | -21.49±0.18   | 44.3 <sup>+3.6</sup> <sub>-4.2</sub>      | 356±46                               | 354±46                           | Sg; Mag99                            |
| N4660          | E                | -5.0±0.5 | 13.2±1.3                      | -18.58±0.21   | 2.41 <sup>+0.55</sup> <sub>-0.68</sub>    | 212±28                               | 213±28                           | Sg; Mag99                            |
| N4874          | E0               | -4.0±0.3 | 100.9±9.8                     | -22.43±0.24   | 225 <sup>+43</sup> <sub>-55</sub>         | 241±31                               | 219±28                           | Sg; Mag99                            |
| N4889          | E4               | -4.0±0.3 | 91.6±8.9                      | -22.32±0.24   | 265 <sup>+55</sup> <sub>-77</sub>         | 381±49                               | 347±45                           | Sg; Mag99                            |
| N6166          | E2pec            | -4.0±0.4 | 131±13                        | -22.85±0.24   | 330 <sup>+41</sup> <sub>-39</sub>         | 326±42                               | 293±38                           | Sg; Mag99                            |
| N7768          | E                | -5.0±0.8 | 114±11                        | -22.22±0.25   | 101 <sup>+20</sup> <sub>-23</sub>         | 232±30                               | 214±28                           | Sg; Mag99                            |
| • Upper Limits |                  |          |                               |               |   |                                      |                                  |                                      |
| N1068          | (R)SA(rs)b       | 3.0±0.3  | 23.6±3.3                      | -20.83±0.58   | <0.16                                     | 153±20                               | 147±19                           | M; G96, Sc00                         |
| N2778          | E                | -5.0±0.8 | 23.3±3.4                      | -18.58±0.34   | <0.49                                     | 173±22                               | 170±22                           | Sg; Mag99                            |
| N3079          | SB(s)c           | 3.0±1.3  | 35±15                         | -19.64±1.06   | <0.022                                    | 150±19                               | 145±19                           | M; T98                               |
| N4151          | E2               | -5.0±0.3 | 16.3±1.5                      | -19.45±0.23   | <12                                       | 178±23                               | 173±23                           | G; W99                               |
| N4203          | SAB0             | -3.0±0.4 | 15.4±1.4                      | -18.64±0.54   | <0.095                                    | 124±16                               | 124±16                           | G; S00                               |
| N4467          | E2               | -5.0±1.0 | 16.7±1.0                      | -16.44±0.20   | <0.30                                     | 86±11                                | 86±11                            | Sg; Mag99                            |

Table 1—Continued

| Galaxy Name | Rev. Hubble Type | T-type   | Distance <sup>(1)</sup> (Mpc) | $B_T^0$ (mag) | BH Mass ( $10^8 M_\odot$ ) | $\sigma^{(2)}$ ( $\text{km s}^{-1}$ ) | $\sigma_c$ ( $\text{km s}^{-1}$ ) | Method and References <sup>(3)</sup> |
|-------------|------------------|----------|-------------------------------|---------------|----------------------------|---------------------------------------|-----------------------------------|--------------------------------------|
| N4945       | SB(s)cd          | 6.0±0.7  | 4.3±0.4                       | -16.37±0.55   | <0.016                     | ...                                   | ...                               | M; GMH97                             |
| N7332       | Lpec             | -2.0±0.3 | 23.5±2.3                      | -19.39±0.55   | <0.081                     | 126±16                                | 124±16                            | Sg; Mag99                            |

<sup>1</sup>Notes on the distances. For lack of independent determinations, distances to Arp102B, NGC 1600, NGC 2300, NGC 2832, NGC 4874, NGC 4889, NGC 6166, NGC 6251, NGC 7052 and NGC 7768 are derived as  $v/H_0$ , where the systemic velocities  $v$  are from the CfA redshift survey (Huchra et al. 1998) and  $H_0 = 71 \pm 7 \text{ km s}^{-1} \text{ Mpc}^{-1}$  (Mould et al. 2000). Of these galaxies, NGC 2300 has  $v \approx 2000 \text{ km s}^{-1}$ , all others have systemic velocities in excess of  $4500 \text{ km s}^{-1}$ , therefore peculiar motions are expected to be negligible. The distance for NGC 224 is from fits to the Cepheid PL relation (Madore & Freedman 1991). The distance to NGC 4258 is geometrically determined from the proper motion of its nuclear water masers (Herrnstein et al. 1999). No direct distances are available for the nearby galaxies NGC 4486B, NGC 4467, NGC 4342, NGC 4945, NGC 4151, NGC 3079 and NGC 1068. For all of them, however, SBF distances are available to nearby companions or members of the same cluster or association. We assume that these galaxies are at the same distance as NGC 4486, NGC 4472, NGC 4472, NGC 5128, NGC 4143, NGC 3073 and NGC 936 respectively. The distance to the galactic center is in kpc (from Genzel et al. 2000)

<sup>2</sup>Notes on the velocity dispersions. All velocity dispersions are from Davies et al. (1987), except for the Milky Way (Kent 1992); NGC 224, NGC1068, NGC 4151 and NGC 4258 (Terlevich et al. 1990); NGC 3079 (Shaw et al. 1993); NGC 4203 and NGC 7332 (Ore 1991); NGC 4594 (De Souza 1993); NGC 6251 (Heckman et al. 1985); NGC 7052 (Wagner 1988). No velocity dispersion data could be found for Arp102B and NGC 4945.

<sup>3</sup>Notes on the BH masses. Codes for the original papers are given in the references. Codes for the methods used in estimating the masses are: G = gas kinematics from HST optical spectra; S = stellar kinematics from HST optical spectra, using axisymmetric dynamical models with 3-integral distribution functions; Sg = stellar kinematics from ground based optical spectra, and/or using isotropic models; M = kinematics of water maser clumps, derived from VLBA data; AD = accretion disk fit to variable H $\alpha$  broad emission lines; PM = proper motion measurements of the SgA star cluster.

Table 2. Results of the Linear Regression Fits:  $Y = \alpha X + \beta$

| X,Y Variables                  | Sample <sup>(1)</sup> | $N$ | $\alpha$   | $\beta$    | $\chi_r^2$ |
|--------------------------------|-----------------------|-----|------------|------------|------------|
| $\log(\sigma_c), \log(M_{BH})$ | A                     | 12  | 5.27±0.40  | -4.04±0.95 | 0.43       |
| $\log(\sigma_c), \log(M_{BH})$ | B                     | 29  | 6.21±0.62  | -5.7±1.4   | 2.8        |
| $\log(v_{rms}), \log(M_{BH})$  | A                     | 10  | 5.93±1.61  | -5.5±3.9   | 8.8        |
| $B_T^0, \log(M_{BH})$          | A                     | 12  | -0.36±0.09 | 1.2±1.9    | 23         |
| $B_T^0, \log(M_{BH})$          | B                     | 30  | -0.48±0.10 | -0.8±2.0   | 25         |

<sup>1</sup>See §3 for a definition of the samples